

# Respiration and Heartbeat Rates Measurement Based on Autocorrelation Using IR-UWB Radar

Hongming Shen, *Member, IEEE*, Chen Xu, Yongjie Yang, Ling Sun, Zhitian Cai, Lin Bai, Edward Clancy, and Xinming Huang, *Senior Member, IEEE*

**Abstract**—Respiration rate (RR) and heartbeat rate (HR) are important physiological parameters for a person. Impulse radio ultra-wideband (IR-UWB) is a promising technology for non-contact sensing and monitoring. This paper presents a new method based on autocorrelation to measure the RR and HR using IR-UWB radar. The correlation coefficient waveform contains the vital sign signals, overcoming the effect of noise and clutter. Applying fast Fourier transform (FFT), the respiration frequency can be acquired easily. A clever method also based on autocorrelation is proposed to locate the subject. The receive signal matrix is divided into a set of bins in the direction of fast time. By removing one block from the matrix each time and re-applying the autocorrelation, the removed block resulting the smallest correlations is corresponding to the location of a subject. Moreover, variational mode decomposition (VMD) algorithm is adopted to successfully separate the respiration and heartbeat signals. Experiments are carried out using a PulsOn410 UWB radar. The results show that the proposed low-complexity algorithm has high accuracy.

**Index Terms**—Respiration rates, heartbeat rates, IR-UWB, autocorrelation, VMD.

## I. INTRODUCTION

RESPIRATION and heartbeat rates are both basic but crucial physiological parameters for human being, especially in medical application, public safety and rescue mission.

Remote sensing with IR-UWB is a promising technology and has gradually been adopted since 2002, when the Federal Communications Commission (FCC) in the United States legalized the microwave range of 3.1G-10.6G Hz for civil purpose [1]. Various applications have been developed using UWB, such as physiological parameter monitoring, through-wall detection, surveillance, real-time localization, robotic arm tracking and microwave imaging [2]. The UWB signal has two sets of definitions: one is defined as fractional bandwidth larger than 20% and the other is defined as absolute bandwidth larger than 500MHz [1]. Comparing with microwave Doppler radar, IR-UWB has the advantages of lower power consumption, smaller size and higher signal-to-noise (SNR), which has the ability of anti-clutter in complex environment [3].

Many research works have been done in the field of UWB remote sensing in the literature. Several works were focused

This work was supported in part by National Students' Platform for Innovation and Entrepreneurship Training Program (201710304051Z), National Natural Science Foundation of China (61571246), Jiangsu Province Prospective Joint Research Project(BY2016053-07).

H. Shen, C. Xu, Y. Yang, L. Sun and Z. Cai are with School of Electronics and Information, Nantong University, Nantong 226019, China. L. Bai, E. Clancy and X. Huang are with Department of Electrical and Computer Engineering, Worcester Polytechnic Institute, MA 01609, USA. The corresponding authors is X. Huang (e-mail: xhuang@wpi.edu).

on improving the hardware or structure of UWB radar, such as improving the radar performance or using multiple radars for complex tasks. In [4], the Tx and Rx antennas were separately placed on the front and back of a human body for better signal penetration. Several works were proposed for signal enhancement, namely raising the signal-to-noise-and-clutter-ratio (SNCR). A method to cancel the respiration-like clutter was presented in [5]. An approach to eliminate the static clutter was presented in [6]. Most of the existing studies put efforts on transformation based algorithm. In [7], conventional FFT was employed to analyze the frequency characteristics of infant respiration. Hilbert-Huang transform (HHT) was used as a time-frequency approach in [8]. Similarly, wavelet transform [9] and short-time Fourier transform (STFT) were adopted to analyze the vital signs in [10], which was able to obtain not only the vital signs but also the spatial distance. There were also plenty of applications developed using IR-UWB, such as through-wall detection [3],[11], movement analysis [12], etc.

In this paper, a novel method based on autocorrelation is proposed for vital sign measurement, including both RR and HR, and also for determining the location. A waveform with high SNCR can be derived directly from the autocorrelation computation, without performing any pre-processing of the original radar data. Applying the conventional FFT method, respiration rate can be easily obtained. In general, heartbeat signal is difficult to detect due to its small amplitude. We propose using the VMD algorithm that can separate center frequencies of RR and HR. In addition, location of a subject is an important parameter. A novel algorithm also based on autocorrelation is proposed in this work. By dividing the radar data matrix into several blocks in fast time direction and moving one block out every time, the autocorrelation coefficient of the remainder matrix in slow time direction can be produced. Subsequently the subject location can be estimated from the correlation results.

The rest of this paper is organized as follows. Section II describes the models of IR-UWB and vital sign signals. In Section III, respiration rate and location estimation algorithms based on autocorrelation are described in details. Furthermore, the VMD method is employed to obtain the heartbeat signal. Experimental results are demonstrated in Section IV and the conclusion is drawn in Section V.

## II. MODEL

### A. IR-UWB Test Setup

Testing environment has critical influence on radar data. For instance, many subjects in the same room can produce multiple

signals at the UWB receiver, so it is difficult to discriminate one signal from others. Strong electromagnetic environment means interference and contamination of signals. To concise the problem and put focus on the scheme and algorithm, a simplified scenario is shown in Fig. 1 [13] where only a single person in a relatively static environment, sitting or standing, faces to the UWB antennas. The distance between the subject and the radar can be adjusted during the experiments.

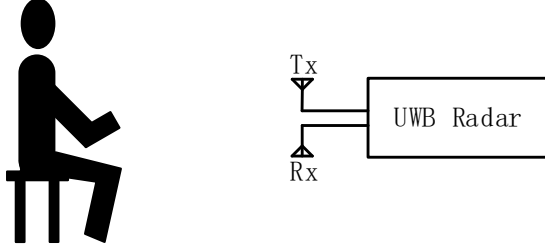


Fig. 1. The basic test scenario with a single person facing the UWB radar

### B. Model of Radar Signal

The operational principle of vital signs remote sensing, such as respiration and heartbeat activities, is based on the detection of UWB pulses reflected from the human body. The amplitude variations as well as the time of arrival (ToA) of the reflected pulse are used to evaluate the motions of the chest and heart, then the status of cardiorespiratory activities can be derived.

When a pulse is transmitted, the radar receives its echoes reflected from the subject. So the distance from the antenna to the subject can be derived as in [3]:

$$\begin{aligned} s(t) &= d_0 + d(t) \\ &= d_0 + d_r \sin(2\pi f_r t) + d_h \sin(2\pi f_h t) \end{aligned} \quad (1)$$

where  $d_0$  is the nominal distance between antenna and human chest wall,  $d_r$  is the displacement amplitude of respiration,  $d_h$  is the displacement amplitude of heartbeat,  $f_r$  represents the respiration frequency and  $f_h$  represents the heartbeat frequency, respectively. The normalized received pulse is denoted by  $\delta(t)$ , and the total impulse response can be represented by:

$$r(t, \tau) = A_k \delta(\tau - \tau_k(t)) + \sum_i A_i \delta(\tau - \tau_i) \quad (2)$$

where  $t$  is the observation time and  $\tau$  is the propagation time.  $A_k \delta(\tau - \tau_k(t))$  denotes the response due to chest wall micro-motion with propagation time  $\tau_k(t)$  and amplitude  $A_k$ .  $\sum_i A_i \delta(\tau - \tau_i)$  denotes the response from kinds of static target with propagation time  $\tau_i$  and amplitude  $A_i$ .  $\tau_k(t)$  is determined by antenna distance  $s(t)$ , and can be expressed as:

$$\begin{aligned} \tau_k(t) &= \frac{2s(t)}{c} \\ &= \tau_0 + \tau_r \sin(2\pi f_r t) + \tau_h \sin(2\pi f_h t) \end{aligned} \quad (3)$$

where  $c$  is the light speed as about  $3 \times 10^8$  m/s,  $\tau_0 = 2s_0/c$ ,  $\tau_r = 2d_r/c$  and  $\tau_h = 2d_h/c$ .

UWB radar converts the received signals into a two-dimension (2D)  $m \times n$  matrix, denoted by  $R[m, n]$ , and it can be expressed as:

$$R[m, n] = r(t = mT_s, \tau = nT_f) \quad (4)$$

where  $m$  and  $n$  represent the sampling numbers in slow time and fast time, respectively.  $T_s$  is the pulse duration in slow time, and  $T_f$  is the fast time sampling interval. Hence, the row vectors record the received signals at different observation time at each range bin while the column vectors record one pulse reflected from different range bin.

Fig. 2 illustrates a respiration model in two directions, i.e. slow time direction and fast time direction, ignoring other signals such as static echoes and clutter. The horizontal axis represents the fast time and the vertical axis represents the slow time. The dashed line frame denotes the subject's position. Note that the periodicity displays not only in the fast time direction due to the pleural periodical movement, but also in the slow time. Time point  $t_0$  and  $(t_0 + T)$  have the similar waveform. It is the basis of the following description.

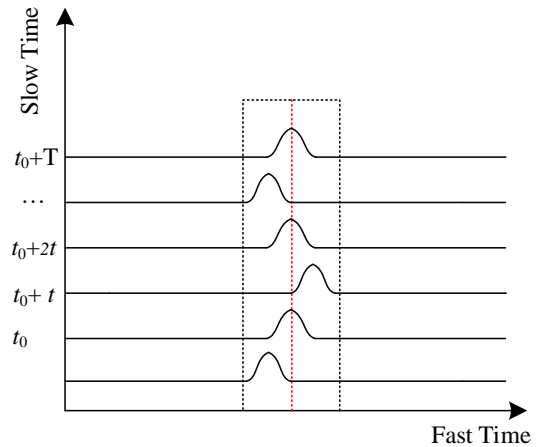


Fig. 2. Slow time and fast time models of radar echoes from pleural periodical movement

## III. SCHEME AND ALGORITHM

### A. Autocorrelation Algorithm

To simplify the problem, both the respiratory signal and the heartbeat signal are generally regarded as periodic sinusoidal signals. Therefore, there are two periodic sinusoidal components in the echoes.

Autocorrelation, also known as serial correlation, is the correlation of a signal with a delay copy of itself as a function of delay. In other words, similarity exists between the observations of the same subject at separate times, and it is a function of time lag. The analysis of autocorrelation is a mathematical tool for finding repeating patterns, such as to find a periodic signal obscured by noise.

The autocorrelation coefficient  $\rho_x(\tau)$  denotes the correlating degree of the same event between two different periods, and the expression is given by:

$$\rho_x(\tau) = \frac{E[(x_i - \mu)(x_{i+\tau} - \mu)]}{\sigma^2} \quad (5)$$

where  $\tau$  is the interval between series  $i_{th}$  and  $(i + \tau)_{th}$ ,  $E$  is the expected value operator,  $\mu$  is the mean value of the series  $x$  and  $\sigma$  is the deviation of  $x$ .

### B. Algorithm for Respiration Rates

In the aforementioned matrix  $R$  each row represents an observation in slow time. As shown in the Fig. 2,  $x(t_0)$  is an observation value at time  $t_0$ , followed with  $x(t_0+t)$ ,  $x(t_0+2t)$ ,  $\dots$ , and so on. Hence, we can get the autocorrelation coefficient between  $x(t_0)$  and  $x(t_0+t)$ ,  $x(t_0)$  and  $x(t_0+2t)$ ,  $\dots$ , and so forth. The autocorrelation coefficient reaches the peak at  $(t_0+T)$  then gradually decreasing, fluctuating as a sine wave, having a same frequency as the humans cardiorespiratory activities. So its periodicity can be represented by  $T$ . Utilizing the FFT method, the respiration frequency can be obtained directly at the maximum value of spectrum due to its highest strength. It is worth noting that data pre-processing is a necessary step to cancel the static component by subtracting the mean value first as shown in (5).

### C. Algorithm for Location

Location of the subject is also an important information, especially in the scenario of disaster rescue. Previously, time-frequency analysis methods, such as wavelet [9] and STFT (short-time Fourier transform) [10] were often been used. In this paper, a novel algorithm also based on autocorrelation is proposed.

All columns in the echo matrix  $R$  are grouped into  $k$  bins of equal sizes. Generally, the size of each bin should be set slightly larger than the thickness of a human body. As shown in Fig. 3, the entire matrix is divided into  $k$  bins, marked in dark color, in the direction of fast time, and the subject should fall into one of these bins which is corresponding to his or her estimated location. Each time we remove one bin out but retain all others in the matrix, and then perform autocorrelation operation similar to obtain the coefficients. Only the largest autocorrelation coefficient is recorded. We repeat the same procedure to remove one bin at a time, sequentially from left to the right. Those recorded maximum autocorrelation coefficients forms a vector. A bin with the smallest value in the vector indicates the location of the subject.

Fig.3 illustrates that the original matrix is separated to  $k$  bins, and the  $j_{th}$  block is moved out. Assuming the subject is located at the  $j_{th}$  block, a significant falling of autocorrelation coefficient should appear because the periodic cardiorespiratory signal with strong correlation has been removed and the remaining noise has poor correlations.

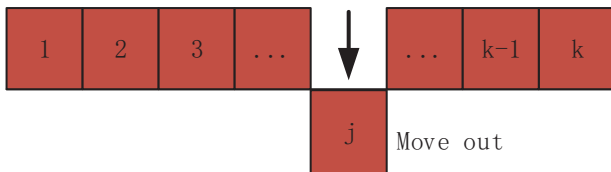


Fig. 3. Illustration of correlation-based location method

### D. Algorithm for Heartbeat Rates

Comparing with respiration signal, heartbeat signal is generally very weak in amplitude. Worse, it is usually close to the high order harmonic of the respiration signal. Therefore, it is very difficult to recognize and distinguish the heartbeat signal from the clutter and noise [14].

VMD is a new algorithm for adaptive data analysis introduced in recent years [15]. By decomposing the input signal into a series of narrow-band components (NBCs) which are concentrated around their corresponding center frequencies, this algorithm can capture the relevant center frequencies quite precisely and identify each dominant mode from the original signal [16].

Computing the bandwidth of NBCs is essentially a constrained variational optimization problem, which is given as follows:

$$\begin{aligned} \min_{\{y_p\}, \{\omega_p\}} \quad & \sum_p \|\partial_t [\delta(t) + \frac{j}{\pi t} \times y_p(t)] e^{-j\omega_p t}\|_2^2 \\ \text{s.t.} \quad & \sum_p y_p(t) = x(t) \end{aligned} \quad (6)$$

where  $\{y_p\} = \{y_1, y_2, \dots, y_p\}$  represents the set of obtained NBCs,  $\{\omega_p\} = \{\omega_1, \omega_2, \dots, \omega_p\}$  represents the corresponding center frequencies,  $\delta(t)$  represents the Dirac distribution function and  $p$  represents the total number of NBCs, respectively. By introducing the Lagrange multiplier  $\lambda$  and penalty factor of reconstruction fidelity term  $\alpha$ , equation (6) can be converted into an unconstrained one as below:

$$\begin{aligned} \mathcal{L}(\{y_p\}, \{\omega_p\}, \lambda) = & \alpha \sum_p \|\partial_t [\delta(t) + \frac{j}{\pi t} \times y_p(t)] e^{-j\omega_p t}\|_2^2 \\ & + \|x(t) - \sum_p y_p(t)\|_2^2 \\ & + \langle \lambda(t), x(t) - \sum_p y_p(t) \rangle \end{aligned} \quad (7)$$

Then the modes  $y_p$  and the associated center frequency  $\omega_p$  can be obtained using an alternating direction method of multipliers approach. Hence, we can get the updated  $y_p(\omega)$  in the  $n_{th}$  cycle by the following as in [17]:

$$\hat{y}_p^{n+1} = \frac{\hat{x}(\omega) - \sum_{i \neq p} \hat{y}_i(\omega) + \frac{\hat{\lambda}(\omega)}{2}}{1 + 2\alpha(\omega - \omega_p)^2} \quad (8)$$

where  $\hat{x}(\omega)$  is the Fourier transform corresponding to  $x(t)$ , and  $\hat{y}_i(\omega)$  is the Fourier transform of  $y_i(t)$  corresponding to the  $i_{th}$  sub-signal. The balancing parameter  $\alpha$  represents the data-fidelity constraint, and it can be taken as a Wiener filter.  $\omega_p$  is updated as:

$$\omega_p^{n+1} = \frac{\int_0^\infty \omega |\hat{y}_p(\omega)|^2 d\omega}{\int_0^\infty |\hat{\mu}_p(\omega)|^2 d\omega} \quad (9)$$

where  $\hat{y}_k(\omega)$  is the Fourier transform of the sub-signal  $y_k(t)$ . The Lagrange multipliers  $\lambda$  is updated as follows, which is useful to exact reconstruction of the input signal:

$$\hat{\lambda}^{n+1}(\omega) \leftarrow \hat{\lambda}^n(\omega) + \beta(\hat{y}(\omega) - \sum_p \hat{y}_p^{n+1}(\omega)) \quad (10)$$

where  $\beta$  is the update parameter of Lagrange multiplier. This process will be terminated once the formula (11) satisfies.

$$\frac{\sum_p \|\hat{y}_p^{n+1} - \hat{y}_p^n\|_2^2}{\|\hat{y}_p^n\|_2^2} < \epsilon \quad (11)$$

where  $\epsilon$  is the tolerance of convergence criterion and the typical value is about  $10^{-6}$ .

Applying the VMD algorithm to the received data  $R$  after pre-processing, respiration and heartbeat frequencies can be measured simultaneously.

#### IV. EXPERIMENTS AND RESULTS

##### A. Hardware Structure

A typical UWB monostatic radar module namely PulsOn 410 is adopted in this experiment. As marked with the dotted line in the Fig. 4, this radar module is composed of many components, including processor, memory, digital baseband, analog front-end, pulser, bandpass filter & LNA, and Tx & Rx antennas. Pulser generates the high frequency pulses and transmits them through Tx antenna under the control of processor. The echoes are received by Rx antenna and processed by processor after a bandpass filter.

The bandwidth of this radar is 2.2 GHz spanning the frequency range of 3.1 to 5.3 GHz, with a center frequency of 4.3 GHz [18]. A Raspberry Pi 3B acts as a core controller that communicates with the radar by a USB cable and collects the raw data from the radar in real-time.

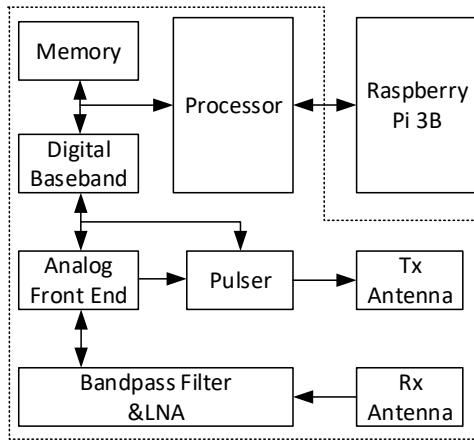


Fig. 4. Block diagram of the IR-UWB radar hardware system

##### B. Data Collection

The sampling frequency is set to 100 Hz. In slow time, 100 observations are recorded per second. Each observation includes 480 sampling values, corresponding to 480 separated bins.

According to the test setup shown in Fig. 1, a person sits on a chair as the test subject, facing to the antenna of the radar. We record a period of 30 seconds each time and sort these data into a two-dimensional  $3000 \times 480$  matrix.

##### C. Bandpass Filter

After removing the static clutter [3], the received echo signal passes through a bandpass filter. The main purpose of the band pass filter is to attenuate signals that are unrelated to cardiorespiratory activities, such as clutter and high frequency component.

The typical respiration frequency and heartbeat frequency of human being are in the range of 0.1-1 Hz and 0.8-2 Hz, respectively. Hence, a 4<sup>th</sup> order Butterworth type bandpass filter with the passband of 0.1-2Hz is designed.

##### D. Measurement Method and Results

Setting the first row of the matrix as the start point, we can calculate the autocorrelation coefficient between this row and each row behind it. A vector of  $1 \times 3000$  is produced and its waveform is shown in Fig. 5. The obvious periodicity can be found, which reveals the periodic vital sign signal. The respiration frequency can be acquired by applying FFT procedure to the waveform. In this example, the RR is about 0.29 Hz as in the spectrogram diagram shown in Fig.6.

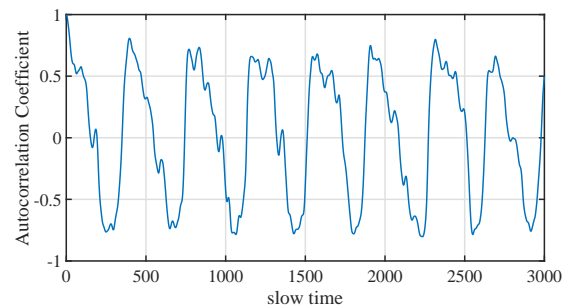


Fig. 5. Autocorrelation coefficient waveform shows the periodic signal

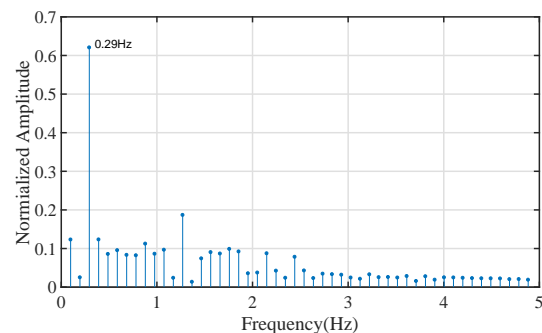


Fig. 6. Spectrogram diagram of vital signs

In order to estimate the subject's location, we divide 480 columns of matrix  $R$  into 12 bins. In our experiment, each column covers about 9.1mm range in space and 40 columns approximately covers the thickness of a normal person. If we remove one bin from  $R$ , the remaining matrix is in the size of  $3000 \times 440$ . Applying the same autocorrelation procedure to the matrix as above, we only record the maximum value of the autocorrelation coefficient. Since we have 12 bins in matrix  $R$ , we can obtain a set of 12 maximum values by removing

one bin at a time. A histogram of these 12 values is plotted as shown in Fig. 7. A small dip is observed at the 5<sup>th</sup> bin, which indicates the location of the subject is in the range of 1.46m-1.82m. The actual distance is 1.65m, appearing as a good estimation of location. By adjusting the locations of the subject, a set of test data is collected as shown in Table 1.

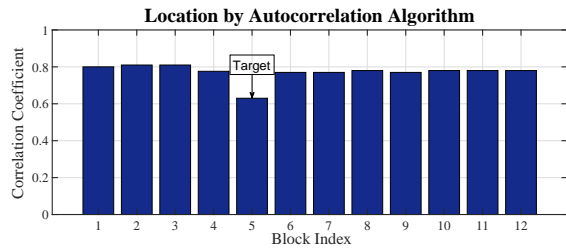


Fig. 7. Location estimation using correlation algorithm

TABLE I  
EXPERIMENTS FOR DIFFERENT SUBJECT LOCATIONS

Actual Distance(m)	Detected Bin Index	Estimation (m)
0.85	3	0.74-1.09
1.32	4	1.09-1.46
1.65	5	1.46-1.82
1.95	6	1.82-2.18
2.32	7	2.18-2.55
2.76	8	2.55-2.91

The data of autocorrelation coefficient are taken as the input parameters of the VMD algorithm. The number of modes is set to 2, corresponding to respiration and heartbeat signals. The balancing parameter and the tolerance are set to 10000 and  $10^{-6}$ , respectively. By applying FFT, the decomposition results are shown in Fig. 8. The respiration frequency is 0.29 Hz, which is the same as direct processing of autocorrelation waveform, and the heartbeat frequency is 1.27 Hz. Correspondingly, the RR can be estimated as 17 times/min and the HR is about 76 beats/min.

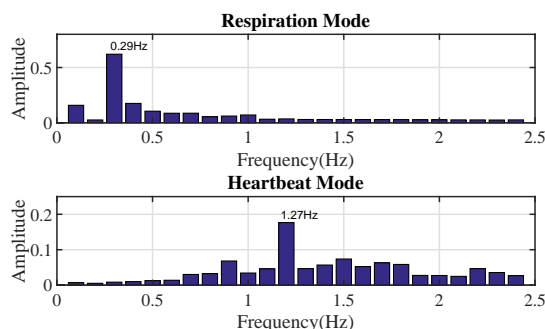


Fig. 8. RR and HR are obtained by VMD algorithm

## V. CONCLUSION

Autocorrelation is a powerful tool to analyze periodical signals. Due to the natural and intrinsic periodicity of vital signs, the autocorrelation method is utilized in this paper,

which provides a simple yet effective solution to IR UWB wireless sensing. Autocorrelation both in slow time and fast time directions are investigated. The respiration frequency and subject location can be acquired accurately from the autocorrelation waveform. The heartbeat frequency can also be derived from the VMD algorithm that can separate the signal from the clutter and noise effectively. This proposed scheme does not require burdensome computation, so it can be efficiently implemented on integrated circuits and embedded systems.

## REFERENCES

- [1] Federal Communications Commission (FCC), "First report and order in the matter of revision of Part 15 of the commissions rules regarding ultra-wideband transmission systems," ET Docket 98-153, FCC 02-48, USA, Apr. 2002.
- [2] W.P. Hung, C.H. Chang, and T.H. Lee, "Real-time and non-contact impulse radio radar system for  $\mu$ m movement accuracy and vital-sign monitoring applications," *IEEE Sensors Journal*, vol. 17, no. 8, pp. 2349-2358, Apr. 2017.
- [3] X. Liang, H. Zhang, G. Fang, S. Ye, and T. A. Gulliver, "An Improved Algorithm for Through-Wall Target Detection Using Ultra-Wideband Impulse Radar," *IEEE Access*, vol. 5, pp. 22101-22118, Nov. 2017.
- [4] Y. Xiong, S. Chen, G. Xing, Z. Peng, and W. Zhang, "Static clutter elimination for FMCW radar displacement measurement based on phasor offset compensation," *Electronics Letters*, vol.53 no.2, pp.1491-1493, Oct. 2017.
- [5] X. Li, Q. Liang, and F. C. M. Lau, "Sense-through-wall human detection using the UWB radar with sparse SVD," *Physical Communication*, vol. 13, pp. 260-266, 2014.
- [6] Z. Li, W. Li, H. Lv, Y. Zhang, X. Jing, and J. Wang, "A novel method for respiration-like clutter cancellation in life detection by dual-frequency IR-UWB radar," *IEEE Trans. Microw. Theory Tech.*, vol. 61, no. 5, pp. 2086-2092, May, 2013.
- [7] X. Huang, L. Sun, T. Tian, Z. Huang, and E. Clancy, "Real-time non-contact UWB radar," in *Proc. IEEE Int. Conf. ICCT*, Oct. 2015, pp. 493-496.
- [8] L. Liu, Z. Liu, H. Xie, B. Barrowes, and A. C. Bagtzoglou, "Numerical simulation of UWB impulse radar vital sign detection at an earthquake disaster site," *Ad Hoc Networks*, vol. 13, pp. 34-41, Feb. 2014.
- [9] Q. An, Z. Li, F. Liang, H. Lv, F. Chen, F. Qi, and J. Wang, "Wavelet based human target detection in complex ruins using a low center frequency uwb radar," in *2016 Progress in Electromagnetic Research Symposium (PIERS)*, Aug. 2016, pp. 1744-1747.
- [10] G. R. Wang, H.G.Han, S. Y. Kim, and T. W. Kim, "Wireless Vital Sign Monitoring Using Penetrating Impulses," *IEEE Microw. Wirel. Components Lett*, vol. 27, no. 1, pp: 94-96, Jan. 2017.
- [11] J. Yan, H. Hong, H. Zhao, Y. Li, C. Gu, and X. Zhu, "Through-Wall Multiple Targets Vital Signs Tracking Based on VMD Algorithm," *Sensors*, vol. 2016, no. 16, pp:1293-1303, Aug. 2016.
- [12] W. P. Hung, C. H. Chang, and T. H. Lee, "Real-time and non-contact impulse radio radar system for m movement accuracy and vital-sign monitoring applications," *IEEE Sens. J.*, vol. 17, no. 8, pp. 2349-2358, Apr. 2017.
- [13] M. Mabrouk, S. Rajan, M. Bolic, M. Forouzanfar, H. R. Dajani, and I. Batkin, "Human Breathing Rate Estimation from Radar Returns Using Harmonically Related Filters," *Journal of Sensors*, vol. 2016, pp. 1-8, 2016.
- [14] W. Yin, X. Yang, L. Zhang, and E. Oki, "ECG Monitoring System Integrated with IR-UWB Radar Based on CNN," *IEEE Access*, vol. 4, pp. 6344-6351, Oct. 2016.
- [15] K. Dragomiretskiy and D. Zosso, "Variational mode decomposition," *IEEE Trans. Signal Process.*, vol. 62, no. 3, pp. 531-544, Feb. 2014.
- [16] A. Upadhyay, and R. B. Pachori, "Speech enhancement based on mEMD-VMD method," *Electron. Lett.*, vol. 53, no. 7, pp: 502-504, Mar. 2017.
- [17] C. Ding, J. Yan, L. Zhang, H. Zhao, H. Hong, and X. Zhu, "Noncontact multiple targets vital sign detection based on VMD algorithm," *2017 IEEE Radar Conference*, Jun. 2017, pp. 727-730.
- [18] Time Domain, "Time domain data sheet of PulsON 400," *Time Domain*, Jun. 2012.